PHYSICAL REVIEW LETTERS **132,** 246901 (2024)

Editors' Suggestion

Analytical Impact-Excitation Theory of Er/O/B Codoped Si Light-Emitting Diodes

Xiaoming Wang,[1] Jiajing He,[1,2] Ao Wang,[3] Kun Zhang,[4] Yufei Sheng,[3] Weida Hu,[4] Chaoyuan Jin,[5] Hua Bao,[3] and Yaping Dan[1,*]

[1]*State Key Laboratory of Advanced Optical Communication Systems and Networks, University of Michigan–Shanghai Jiao Tong University Joint Institute, Shanghai Jiao Tong University, Shanghai 200240, China*

[2]*Aerospace Laser Technology and System Department, Shanghai Institute of Optics and Fine Mechanics, Chinese Academy of Sciences, Shanghai 201800, China*

[3]*Global Institute of Future Technology, Shanghai Jiao Tong University, Shanghai 200240, China*

[4]*State Key Laboratory of Infrared Physics, Shanghai Institute of Technical Physics, Chinese Academy of Sciences, 500 Yu Tian Road, Shanghai 200083, China*

[5]*College of Information Science and Electronic Engineering, Zhejiang University, Hangzhou 310007, China*

(Received 15 February 2024; accepted 8 May 2024; published 11 June 2024)

Er doped Si light-emitting diodes may find important applications in silicon photonics and optical quantum computing. These diodes exhibit an emission efficiency 2 orders of magnitude higher at reverse bias than forward bias due to impact excitation. However, physics of impact excitation in these devices remains largely unexplored. In this work, we fabricated an Er/O/B codoped Si light-emitting diode which exhibits a strong electroluminescence by the impact excitation of electrons inelastically colliding the Er ions. An analytical impact-excitation theory was established to predict the electroluminescence intensity and internal quantum efficiency which fit well with the experimental data. From the fittings, we find that the excitable Er ions reach a record concentration of 1.8×10^{19} cm^{-3} and up to 45% of them is in an excitation state by impact excitation. This work has important implications for developing efficient classical and quantum light sources based on rare earth elements in semiconductors.

DOI: 10.1103/PhysRevLett.132.246901

An integrated chip system that possesses the generation [1], processing [2,3], transmission, and storage of quantum information [4] is vital for quantum computing, in particular if such a system can be integrable with the existing Si based complementary-metal-oxide-semiconductor (CMOS) circuitry. Er ions implanted in silicon provide an unprecedented opportunity to develop such a system due to several important features of Er ions [5–7]. First, Er ions absorb or emit photons at a communication wavelength that is compatible with the existing optical communication systems and the emerging silicon photonic technology [8,9]. Second, rare earth elements in crystals often have a long spin coherent time [10], a striking feature that is crucial for quantum information processing. Er as one of the most extensively investigated rare earth elements is not an exception. Last, Er ions have a longitudinal spin wave structure which can be coupled with electromagnetic waves in a microwave or radio frequency range [11]. As a result, the electron spin coherence in Er ions can be manipulated optically and electronically [10,12,13].

In the past several decades, Er in various substances has been well studied including crystalline and nanostructured semiconductors and dielectrics [14–18]. The research on Er in oxide or other dielectrics is fruitful, partly because Er has a high solubility in these materials [15,16]. A high concentration of these Er ions can be directly excited by photons with the right energy. Optically pumped lasers and optical amplifiers based on Er doped fibers have been commercialized. The pursuit of electrically pumped Er doped Si light-emitting devices operating at a forward bias turns out to be futile due to the fact that Er ions in these devices are excited by the recombination of electrons and holes from the energy bands via Er-related defects in the Si band gap, which often results in an extremely low efficiency [5].

Impact excitation provides a new avenue for creating efficient Er-doped Si light-emitting diodes (LEDs) [19,20]. Like optical pumping, impact excitation can provide tunable quantized energies by the electric field in the depletion region of the *p*-*n* junction diode in which electrons are ballistically accelerated within the mean free path and inelastically collide to excite Er ions. Er doped Si LEDs under reverse bias were previously reported to have much higher luminescence intensities than forward bias [19,20], which was believed to be caused by impact excitation. However, the physics of impact excitation has remained largely unexplored.

In this work, we fabricated an Er/O/B codoped Si LED that exhibits an electroluminescence (EL) emission 2 orders of magnitude stronger at reverse bias than forward bias.

 © 2024 American Physical Society

The derived impact-excitation theory predicts that the emission rate and internal quantum efficiency (IQE) follow the nonlinear functions of reverse bias, which, excitingly, was consistent with experimental observations. The fitting of the theory with the roughly estimated IQE allows us to find that the optical excitable Er concentration reaches a record of 1.8×10^{19} cm^{-3}, 45% of which is excited at a reverse bias of 11 V. This ratio can be enhanced toward 100% by increasing the pumping current or reducing the Er concentration, which is important for developing single photon sources when a single Er is introduced into Si.

The intrinsic silicon wafer (p type; resistivity ≥ 10 kΩ cm) was first doped with Er and O at an implantation energy and dose of 200 keV and 4×10^{15} cm^{-2}, and 30 keV and 1×10^{16} cm^{-2}, respectively. Photolithography was applied to expose part of Er/O codoped Si which was further implanted with boron at 20 keV and 1×10^{15} cm^{-2}. After ion implantation, the sample was then treated with the deep cooling process in which the sample was rapidly quenched from high temperature (950 °C) by flushing with helium gas cooled with liquid nitrogen (77 K). Hall measurements show that the Er/O doped Si is n type with the electron concentration of $\sim 1 \times 10^{19}$ cm^{-3}, whereas the Er/O/B doped Si is p type with the hole concentration of $\sim 4.7 \times 10^{18}$ cm^{-3}. See Supplemental Material for Hall measurements [21]. We previously demonstrated that the deep cooling process can efficiently suppress the precipitation of Er and reduce the concentration of nonradiative recombination centers [23], as a result of which the Er/O doped Si has a 2-order-of-magnitude enhancement of light emission efficiency. The codoping of B will further enhance the photoluminescence efficiency of Er/O doped Si. (The photoluminescence for Er/O and Er/O/B doped Si is presented in Fig. S1c of Supplemental Material [21].)

We made a cross-finger shaped p-n junction diode as shown in Fig. 1(a). A pair of cross-finger electrodes were deposited to contact the n^+-type Er/O and p^+-type Er/O/B region, respectively. The contacts are Ohmic and the contact resistances are negligible in comparison with the resistance of the p-n junction at reverse bias. (The contact resistances were extracted from the transmission line model in Fig. S2 of Supplemental Material [21].) The current vs voltage (I-V) characteristics of the p-n junction diode are shown in Fig. 1(b). The leakage current is relatively large with only an order of magnitude lower than the forward current. The relatively large leakage current is likely due to the high concentration of defects by Er/O/B doping that significantly increases the thermal generation of electrons and holes in the depletion region. The ideality factor is found as ~2.7 from the slope of the logarithmic forward current at small forward bias [inset of Fig. 1(b)].

The electroluminescence (EL) spectra of the p-n junction diode under forward (blue line) and reverse bias (red line) are shown in Fig. 1(c). Both spectra exhibit a peak near 1.536 μm which is nearly identical to the recorded

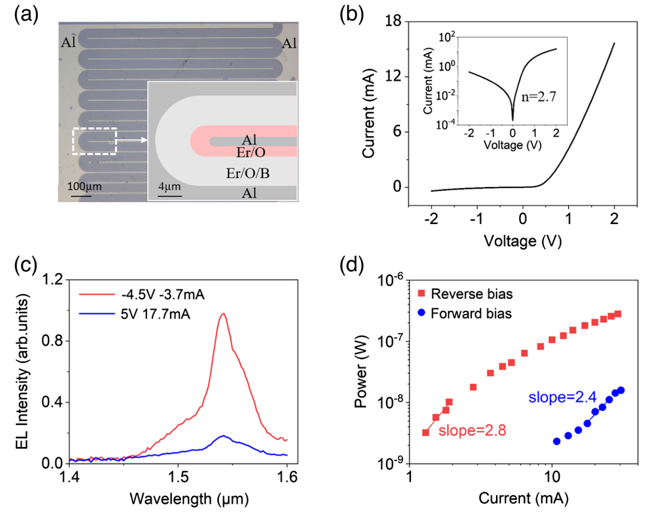

FIG. 1. (a) Optical microscopic image of the device. Inset: A closeup sketch of p-n junction. (b) Current vs voltage (I-V) characteristics of the Er/O/B codoped Si p-n junction. Inset: I-V characteristics in semilogarithmic scale. (c) EL spectra under reverse and forward bias. (d) Photo emission power under the injection of different currents at room temperature.

photoluminescence (PL) of Er/O codoped Si ([21], Fig. S1c) confirming that the EL emission comes from Er ions. Figure 1(d) shows the integrated EL intensity pumped by a forward (blue dots) and a reverse current (red squares). The EL under reverse bias is nearly 2 orders of magnitude stronger than the forward bias. Interestingly, the dependence of EL intensity on pump current has a slope of 2.4–2.8, indicating that there is some stimulated emission inside the diode. We previously observed similar phenomenon in other Er doped Si light-emitting diodes [7].

The strong EL under reverse bias is caused by impact excitation of hot electrons. To theoretically investigate this impact-excitation process, let us focus on electrons in the depletion region starting from the location ① in thermal equilibrium (see Fig. 2). Within a distance of the mean free path, the electrons will ballistically transport until they collide the impurity ions (mostly Er ions). In our case, the depletion region width is estimated to be ~45 nm due to the lateral randomness of implanted ions. (The lateral distribution of implanted ions is shown in Fig. S3 of Supplemental Material [21].) EL from our p-n junction diode was detectable when the reverse bias is greater than 3 V. The maximum electric field intensity inside the depletion region is on an order of 10^6 V/cm, meaning that some electrons in the depletion region have already reached the velocity saturation according to the electric field dependent velocity of electrons in silicon. Therefore, electrons will mostly inelastically collide with impurities at the location ② after traveling a distance of mean free path (~4 nm from our later results). Given the fact that the time of ballistic transport is on the order of ~tens of femtoseconds, electrons before collision are hot electrons with a

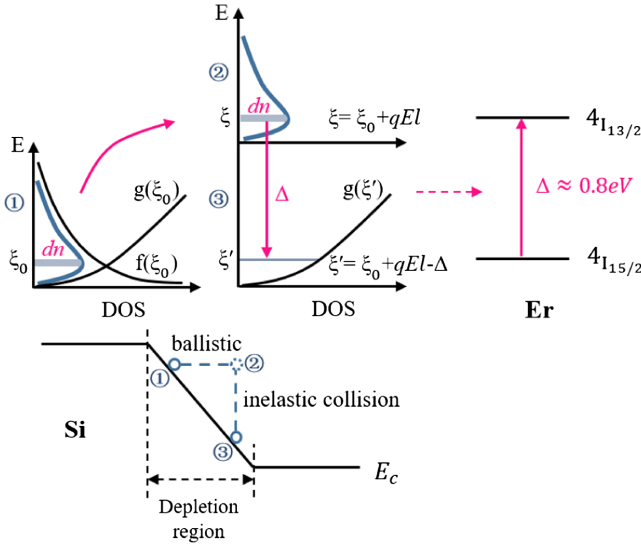

FIG. 2. Impact-excitation mechanism. Electrons in the location ① will be ballistically accelerated to the location ② in a short time (∼tens of femtoseconds) such that the hot electrons in the location ② distribute identically to the location ①. After the inelastic collision, those electrons lose an energy of Δ that will be absorbed by Er ions to excite electrons from the ground state to excited state.

distribution similar to ① but at a higher energy of qEl with q being the unit charge, E the electric field intensity, and l the mean free path. After collision, electrons will relax to empty states at ③.

Electrons of Er ions at $^4I_{15/2}$ states are excited to $^4I_{13/2}$ states only if hot electrons at $\xi = \xi_0 + qEl$ in ② are relaxed by inelastic collision to states at ξ' (mostly empty in ③) by losing an energy of Δ ($\cong 0.8$ eV). For all electrons in the location ②, the probability W_i of an Er ion being excited is given by Eq. (1) according to previous theoretical work [24].

$$W_i = W_0 \iint_{\xi_0 \geq 0, \xi' \geq 0} g(\xi) f(\xi) g(\xi') \delta(\xi - \Delta - \xi') \, d\xi d\xi', \quad (1)$$

in which $\xi = \xi_0 + qEl$, W_0 is associated with the Er ion radius and Coulombic interactions (1.4×10^{-9} cm^{-3} eV$^{-1/2}$ s^{-1}) [22], g is the density of states, and f is the carrier distribution function. Since the free carrier concentration in the depletion region is relatively low, f will follow the Boltzmann distribution although the Si is degenerate due to high doping concentrations. The last term $\delta(\xi - \Delta - \xi')$ in the integral is to ensure that the energy loss in the inelastic collision matches the energy needed for electrons in Er ion to excite from $^4I_{15/2}$ to $^4I_{13/2}$ states.

Depending on whether the kinetic energy is higher or lower than the energy difference Δ, the probability of impact excitation W_i given in Eq. (2) can be derived from Eq. (1) [24] [Eqs. (1) and (2) are validated numerically in Sec. IV of Supplemental Material [21]] where n is the hot electron concentration, k is the Boltzmann constant, and T is the electron temperature. In our case, the kinetic energy of electrons is higher than 0.8 eV (see later results). Therefore, we focus only the case $qEl \geq \Delta$ in Eq. (2) for the following derivation.

$$W_i = \begin{cases} \frac{W_0}{\pi} n \sqrt{qEl - \Delta} & qEl \geq \Delta\,, \\ \frac{W_0}{\pi} n \sqrt{\Delta - qEl}\; e^{-\frac{\Delta - qEl}{kT}} & qEl \leq \Delta\,. \end{cases} \quad (2)$$

Note that the electric field intensity and dopants in our p-n junction are not spatially uniform, and that the emission probability W_i is dominated by the maximum electric field intensity. For simplicity, we choose to use the maximum electric field intensity E_m in Eq. (2) for a given reverse bias V_a, which is written as $E_m = \{[2(V_{bi} + V_a)]/W_{\rm dep}\}$ with V_{bi} being the built-in potential (∼1.06 V), and $W_{\rm dep}$ is the depletion region width. $W_{\rm dep}$ is ∼45 nm estimated from the lateral randomness of ion implanted dopants and regarded as constant due to the fact that both Er/O/B and Er/O doped Si are degenerate ([21], Fig. S3).

In Eq. (2), the electron concentration n is also dependent on the reverse bias V_a. Since the electrons in the depletion region under a reverse bias of 3 V have already reached the velocity saturation in our device, the electron concentration n can be expressed in terms of leakage current density J and electron saturation velocity v_s as $n = (J/qv_s)$. The experimental leakage current and then the electron concentration can be fitted with an exponential function of reverse bias V_a as shown in Fig. 3(a). After plugging the analytical dependence of n and E on V_a into Eq. (2), we manage to find the analytical expression of W_i dependent on V_a which is plotted in Fig. 3(b).

Note that the kinetic energy of inelastic collision can be transferred only to Er ions that are not in excitation state (in ground state). Let us suppose the concentration of all optically excitable Er ions and those already in excitation state are N_{tt} and $N_{\rm Er}$, respectively. Er ions in ground state will be $N_{tt} - N_{\rm Er}$ in concentration. The radiative emission probability of Er ions in the excitation state is W_d. At steady state, the excitation rate of Er ions in ground state by inelastic collision of hot electrons will be equal to the relaxation rate of Er ions from excitation state to ground state, which can be described by Eq. (3).

$$W_i(N_{tt} - N_{\rm Er}) = N_{\rm Er} W_d. \quad (3)$$

From Eq. (3), we find the concentration of Er ions in excitation state $N_{\rm Er}$ with the expression of W_i given in Eq. (2). The photon emission rate r_e from our Er doped Si is given by $r_e = N_{\rm Er} W_d L_{ex} A_c$ where A_c is the cross-sectional area of the conduction channel with the cross-finger interface length of 1 cm and depth of 100 nm according to the doping profile (see Supplemental Material, Sec. I).

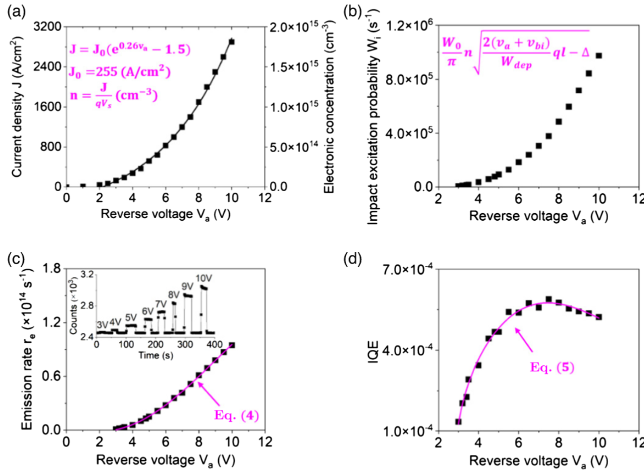

FIG. 3. (a) Experimental leakage current density that is exponentially dependent on reverse bias V_a which can be fitted with an empirical function. (b) Photo emission probability due to impact excitation by plugging the measured electron concentration in (a) to Eq. (2). (c) Emission rate as a function of reverse bias V_a. Inset: EL under a pulsed bias to mitigate thermal effect. (d) Experimentally measured IQE that is well fitted with the theoretical IQE in Eq. (5).

L_{ex} is the length of the optically active region (should be around where the maximum electric field intensity is). The full expression of r_e is given as a function of reverse bias V_a in Eq. (4) after plugging N_{Er} found from Eq. (3), the empirical expression of the electron concentration in Fig. 3(a) and W_i given in Eq. (2) along with the maximum electric field intensity.

$$r_e = \frac{W_i}{W_i + W_d} N_{tt} W_d L_{ex} A_c = \frac{J\sqrt{V_a + V_{bi} - A}}{J\sqrt{V_a + V_{bi} - A} + B/J_0} N_{tt} W_d L_{ex} A_c, \qquad (4)$$

in which $A = (W_{\mathrm{dep}}/2ql)\Delta$ and $B = (\pi v_s W_d / W_0) \times \sqrt{(qW_{\mathrm{dep}}/2l)}$.

To quantitatively measure the photon emission rate r_e from our reversely biased p-n junction diode, we used a commercially calibrated near-infrared light-emitting diode (InGaAs diode L12509-0155G) as a reference to quantify the light collection efficiency of our optical system. (The system optical collection efficiency was experimentally measured as shown in Fig. S5 of Supplemental Material [21].) Silicon has a relatively high refractive index. Light emitted from Si internally may be trapped inside. Based on finite difference time domain simulations, we found the light extraction efficiency from silicon to air is estimated as 2.3% to the best of our knowledge. Note this efficiency may bear some significant uncertainty that will affect the value of the parameters we extracted below. With these considerations, we recorded the photon emission rate r_e from our device at pulsed bias to mitigate the thermal effect, as shown in Fig. 3(c) along with the inset.

The experimentally measured photon emission rate can be fitted with the theoretical rate given in Eq. (4). From the fitting, we extracted three important correlations given $V_{bi} = 1.06$ V. First, $A = (W_{\mathrm{dep}}/2ql)\Delta = 4.3$ V with l being the mean free path and $\Delta = 0.8$ eV, from which we find $(W_{\mathrm{dep}}/l) = 11$. As W_{dep} can be reliably estimated as ∼45 nm from the SRIM simulation of dopant distribution (Fig. S3 in [21]), we conclude that the electron mean free path in our sample is ∼4 nm, which is consistent with the results in literature [25]. Second, $(B/J_0) = (\pi v_s W_d / W_0 J_0) \times \sqrt{(qW_{\mathrm{dep}}/2l)} = 31\ V^{-1/2}$ from which we find $W_d = 1 \times 10^6\ \mathrm{s}^{-1}$ given $J_0 = 255\ \mathrm{A/cm}^2$ from the experimental current fitting in Fig. 3(a), $W_0 = 1.4 \times 10^{-9}\ \mathrm{cm}^{-3}\,\mathrm{eV}^{-1/2}\,\mathrm{s}^{-1}$ given in Eq. (1) and v_s the electron saturation velocity that often equals to $\sim 10^7$ cm/s in silicon [26]. The extracted W_d is 2–3 orders of magnitude larger than what we found optically. (The optical emission probability W_d can be found by fitting the transient decay PL with a stretched exponential function as shown in Fig. S1d of Supplemental Material [21].) This is either because strong electric fields can enhance the emission probability of excited Er ions or due to the overestimation of leakage current. The third important correlation is $N_{tt} W_d L_{ex} A_c = 1.9 \times 10^{14}\ \mathrm{s}^{-1}$ in which L_{ex} is the length of optically active region. The depletion region is ∼45 nm wide and L_{ex} is part of it. On the other hand, L_{ex} should be longer than the electron mean-free path which is ∼4 nm. Therefore, it is reasonable to set L_{ex} as ∼10 nm. Based on these estimated parameters, we find $N_{tt} = 1.9 \times 10^{19}\ \mathrm{cm}^{-3}$. Secondary ion mass spectrometry shows the maximum Er doping concentration in our device is $\sim 7 \times 10^{20}\ \mathrm{cm}^{-3}$. (The doping profile of Er, O, and B are shown in Fig. S1 of Supplemental Material [21].) This indicates that only 2.5% of implanted Er ions are optically active, which is consistent with our previous finding by optical excitation [22]. Among these $1.9 \times 10^{19}\ \mathrm{cm}^{-3}$ optically excitable Er ions, up to ∼45% $(8.1 \times 10^{18}\ \mathrm{cm}^{-3})$ of them are in an excited state at a maximum reverse bias of $V_a = 11$ V. According to the theory, it can be predicted that a further increase in the bias voltage will increase the number of Er ions in excited state although the IQE will decrease. For example, it is not difficult to find that ∼90% optically excitable Er ions will be in an excitation state at a bias of 18.5 V. To summarize, we listed in the table of Supplemental Material, Sec. VI [21] some known parameters from other sources and those extracted from our fittings.

The number of electrons injected into the reverse biased p-n junction diode per second is given by JA_c/q where J is the leakage current density, A_c is the cross-section area of the conduction channel, and q is the

unit of charge. The IQE is given by the ratio of r_e to JA_c/q as shown in Eq. (5).

$$\mathrm{IQE} = \frac{N_{Er} W_d L_{ex} A_c}{J A_c / q} = \frac{\frac{W_0}{\pi} n \sqrt{q E_m l - \Delta}}{\frac{W_0}{\pi} n \sqrt{q E_m l - \Delta} + W_d} \frac{q N_{tt} W_d L_{ex}}{J}, \tag{5}$$

in which L_{ex} is the length of optically active region and v_s is the saturation velocity of electrons. IQE in Eq. (5) becomes an explicit function of V_a after plugging the empirical expression of J given in Fig. 3(a) with $n = (J/qv_s)$ and the maximum electric field intensity dependent on V_a.

Figure 3(d) plots the experimentally measured IQE as a function of reverse bias voltage. IQE increases from 3 V and starts to drop after reaching the maximum at ∼7 V. Amazingly, this nonlinear dependence of IQE on V_a can be nicely fitted with Eq. (5). From the fitting, we extracted the parameters that are the same with those from the previous fitting of the theoretical emission rate with the experimental rate in Fig. 3(c).

In the end, we need to point out that the increase of optically active Er ions in the depletion region helps to enhance the IQE. One possible approach is to reduce the free carrier concentration of Er/O/B doped Si by fine-tuning the boron dose so that this Er/O/B region has a low concentration of free charge carriers. Under reverse bias, the whole quasi-intrinsic Er/O/B region can be depleted with a high electric field inside, which will significantly increase the emission efficiency.

On the other hand, we can reduce the concentration of Er ions in the optically active region to create a quantum light source. For example, if there is only one optically active Er ion in the depletion, a steady state of Eq. (3) cannot be established, meaning that the only Er ion is either in the ground state to zero out the right side of Eq. (3) or in excitation state to zero out the left side. To maintain a stable periodic flip-flop state (periodic single photon emission), it is required to have $W_i \geq W_d$. In our case, the impact-excitation probability W_i reaches $1 \times 10^6\ \mathrm{s}^{-1} = W_d$ at a bias of 10 V [Fig. 3(b)]. Since such a single photon source is in silicon, it therefore can be monolithically integrated with silicon waveguide, modulators, photodetectors, and CMOS transistors for developing silicon quantum photonics.

Conclusion.—In this work, we fabricated an Er doped Si light-emitting diode with Er/O and Er/O/B as the n^+ and p^+ region, respectively. The EL emission at 1.536 μm from the depletion region of the Si diode is enhanced by 2 orders of magnitude under reverse bias. The internal quantum efficiency (IQE) exhibits a nonlinear dependence on reverse bias, which increases with reverse bias but starts to decline after reaching a maximum IQE of 0.06% at 7 V. To theoretically analyze the EL emission, we developed an impact-excitation theory for hot electrons with high kinetic energy to excite Er ions by inelastic collision. This theory allows us to establish a theoretical IQE that fits well with the experimentally measured nonlinear IQE. From the fitting, we find that ∼45% of the optically active Er ions are excited by impact excitation, which can be further increased by increasing the pumping current. The theory also predicts that a single photon emitter can be built if there is only one optically active Er ion in the depletion at a condition of the impact-excitation probability greater than the radiative emission probability of Er ions. Although the impact-excitation theory is derived for Er ions in Si, it can be generalized for radiative rare earth elements and defects in semiconductors by impact excitation.

This work was financially supported by the special-key project of Innovation Program of Shanghai Municipal Education Commission (No. 2019-07-00-02-E00075), National Science Foundation of China (NSFC, No. 92065103 and No. 62305354), Oceanic Interdisciplinary Program of Shanghai Jiao Tong University (SL2022ZD107), Shanghai Jiao Tong University Scientific and Technological Innovation Funds (2020QY05), and Shanghai Pujiang Program (22PJ1408200). The devices were fabricated at the center for Advanced Electronic Materials and Devices (AEMD), and PL and Hall effect measurements were carried out at the Instrumental Analytical Center (IAC), Shanghai Jiao Tong University.

[*]Corresponding author: Yaping.dan@sjtu.edu.cn

[1] Z. Zhou *et al.*, On-chip light sources for silicon photonics, Light **4**, e358 (2015).
[2] C. D. Bruzewicz, J. Chiaverini, R. McConnell, and J. M. Sage, Trapped-ion quantum computing: Progress and challenges, Appl. Phys. Rev. **6**, 021314 (2019).
[3] J. Wang, F. Sciarrino, A. Laing, and M. G. Thompson, Integrated photonic quantum technologies, Nat. Photonics **14**, 273 (2020).
[4] G. Zhang *et al.*, An integrated silicon photonic chip platform for continuous-variable quantum key distribution, Nat. Photonics **13**, 839 (2019).
[5] A. Kenyon, Erbium in silicon, Semicond. Sci. Technol. **20**, R65 (2005).
[6] Y. Liu *et al.*, A photonic integrated circuit–based erbium-doped amplifier, Science **376**, 1309 (2022).
[7] J. Hong, H. Wen, J. He, J. Liu, Y. Dan, J. W. Tomm, F. Yue, J. Chu, and C. Duan, Stimulated emission at 1.54 μm from erbium/oxygen-doped silicon-based light-emitting diodes, Photonics Res. **9**, 714 (2021).
[8] B. Wang, P. Zhou, and X. Wang, Recent progress in on-chip erbium-based light sources, Appl. Sci. **12**, 11712 (2022).
[9] J. C. Palais, *Fiber Optic Communications* (Prentice-Hall, Inc., 1984).
[10] M. Le Dantec *et al.*, Twenty-three–millisecond electron spin coherence of erbium ions in a natural-abundance crystal, Sci. Adv. **7**, eabj9786 (2021).

[11] V. Buchel'nikov, I. V. Bychkov, Y. A. Nikishin, S. B. Palmer, C. M. Lim, and C. Edwards, Electromagnetic-acoustic transformation in an erbium single crystal, Phys. Solid State **44**, 2116 (2002).

[12] H.-J. Lim, S. Welinski, A. Ferrier, P. Goldner, J. J. L. Morton, Coherent spin dynamics of ytterbium ions in yttrium orthosilicate, Phys. Rev. B **97**, 064409 (2018).

[13] A. Ortu, A. Tiranov, S. Welinski, F. Fröwis, N. Gisin, A. Ferrier, P. Goldner, and M. Afzelius, Simultaneous coherence enhancement of optical and microwave transitions in solid-state electronic spins, Nat. Mater. **17**, 671 (2018).

[14] A. Kenyon, Recent developments in rare-earth doped materials for optoelectronics, Prog. Quantum Electron. **26**, 225 (2002).

[15] H. Sun, L. Yin, Z. Liu, Y. Zheng, F. Fan, S. Zhao, X. Feng, Y. Li, and C. Z. Ning, Giant optical gain in a single-crystal erbium chloride silicate nanowire, Nat. Photonics **11**, 589 (2017).

[16] M. Miritello, R. Lo Savio, F. Iacona, G. Franzò, A. Irrera, A. M. Piro, C. Bongiorno, and F. Priolo, Efficient luminescence and energy transfer in erbium silicate thin films, Adv. Mater. **19**, 1582 (2007).

[17] M. A. Lamrani, M. Addou, Z. Sofiani, B. Sahraoui, J. Ebothé, A. El Hichou, N. Fellahi, J. C. Bernède, and R. Dounia, Cathodoluminescent and nonlinear optical properties of undoped and erbium doped nanostructured ZnO films deposited by spray pyrolysis, Opt. Commun. **277**, 196 (2007).

[18] F. Priolo, G. Franzò, S. Coffa, A. Polman, S. Libertino, R. Barklie, and D. Carey, The erbium-impurity interaction and its effects on the 1.54 μm luminescence of Er^{3+} in crystalline silicon, J. Appl. Phys. **78**, 3874 (1995).

[19] S. Harako *et al.*, Visible and infrared electroluminescence from an Er-doped n-ZnO/p-Si light emitting diode, Phys. Status Solidi (a) **205**, 19 (2008).

[20] G. Franzò, S. Coffa, F. Priolo, and C. Spinella, Mechanism and performance of forward and reverse bias electroluminescence at 1.54 μm from Er-doped Si diodes, J. Appl. Phys. **81**, 2784 (1997).

[21] See Supplemental Material at http://link.aps.org/supplemental/10.1103/PhysRevLett.132.246901, which includes Refs. [22], for additional information about the experimental methods, Hall measurements, calibration of optical collection efficiency, and table for extracted parameters.

[22] H. Liu *et al.*, Quantification of energy transfer processes from crystalline silicon to erbium, J. Mater. Chem. C **11**, 2169 (2023).

[23] H. Wen, J. He, J. Hong, S. Jin, Z. Xu, H. Zhu, J. Liu, G. Sha, F. Yue, and Y. Dan, Efficient Er/O-doped silicon light-emitting diodes at communication wavelength by deep cooling, Adv. Opt. Mater. **8**, 2000720 (2020).

[24] I. Yassievich and L. Kimerling, The mechanisms of electronic excitation of rare earth impurities in semiconductors, Semicond. Sci. Technol. **8**, 718 (1993).

[25] B. Qiu Z. Tian, A. Vallabhaneni, B. Liao, J. M. Mendoza, O. D. Restrepo, X. Ruan, and G. Chen, First-principles simulation of electron mean-free-path spectra and thermoelectric properties in silicon, Europhys. Lett. **109**, 57006 (2015).

[26] K. Seeger, *Semiconductor Physics* (Springer Science & Business Media, New York, 2013).